Applied and Environmental Microbiology, Aug. 2009, p. 5218–5226 Vol. 75, No. 16
0099-2240/09/$08.00+0 doi:10.1128/AEM.00544-09

Kinetic Characterization of OmcA and MtrC, Terminal Reductases Involved in Respiratory Electron Transfer for Dissimilatory Iron Reduction in *Shewanella oneidensis* MR-1[▽]

Daniel E. Ross,[1,2] Susan L. Brantley,[1,3] and Ming Tien[1,2]*

Center for Environmental Kinetics Analysis,[1] Department of Biochemistry and Molecular Biology,[2] and Earth and Environmental Systems Institute,[3] The Pennsylvania State University, University Park, Pennsylvania 16802

Received 6 March 2009/Accepted 11 June 2009

We have used scaling kinetics and the concept of kinetic competence to elucidate the role of hemeproteins OmcA and MtrC in iron reduction by *Shewanella oneidensis* MR-1. Second-order rate constants for OmcA and MtrC were determined by single-turnover experiments. For soluble iron species, a stopped-flow apparatus was used, and for the less reactive iron oxide goethite, a conventional spectrophotometer was used to measure rates. Steady-state experiments were performed to obtain molecular rate constants by quantifying the OmcA and MtrC contents of membrane fractions and whole cells by Western blot analysis. For reduction of soluble iron, rates determined from transient-state experiments were able to account for rates obtained from steady-state experiments. However, this was not true with goethite; rate constants determined from transient-state experiments were 100 to 1,000 times slower than those calculated from steady-state experiments with membrane fractions and whole cells. In contrast, addition of flavins to the goethite experiments resulted in rates that were consistent with both transient- and steady-state experiments. Kinetic simulations of steady-state results with kinetic constants obtained from transient-state experiments supported flavin involvement. Therefore, we show for the first time that OmcA and MtrC are kinetically competent to account for catalysis of soluble iron reduction in whole *Shewanella* cells but are not responsible for electron transfer via direct contact alone with insoluble iron-containing minerals. This work supports the hypothesis that electron shuttles are important participants in the reduction of solid Fe phases by this organism.

Microbial processes play a central role in the cycling of organic and inorganic compounds on Earth. A select number of these compounds are assimilated by organisms and used as building material for the cell. In addition, a large number of organic and inorganic compounds are used as electron donors and acceptors for respiratory metabolism. Iron, one of the most abundant elements in the Earth's crust, is both assimilated by life and utilized as an electron donor (Fe^{2+}) and acceptor (Fe^{3+}) in respiratory metabolism. Due to the importance of iron, microorganisms directly impact the fate and transport of iron, and these Fe impacts indirectly influence the (bio)geochemical cycles of many other elements, including the carbon cycle (38). Furthermore, respiratory metabolism evolved in microorganisms prior to the emergence of oxygenic photosynthesis and was very versatile in using a large number of both organic and inorganic terminal electron acceptors (TEAs) (29). Therefore, the use of iron as a TEA predates the use of molecular oxygen among organisms on Earth. When metals are used as the TEA, this process is referred to as dissimilatory metal reduction (DMR) or, in the case of iron, dissimilatory iron reduction (DIR). Interest in microbial DMR has intensified upon discovery of the ability of DMR bacteria to catalyze reactions of environmentally relevant contaminants, including radionuclides such as U(VI) (1, 19, 20, 24, 30, 45, 47).

DMR has been extensively studied in the facultative anaerobe *Shewanella oneidensis* MR-1 due to its respiratory versatility (for a review, see references 22, 23, 39, and 49). This bacterium also has the ability to utilize soluble and insoluble forms of iron and manganese as TEAs (12, 17, 25, 29, 33, 36). Genetic and biochemical studies show that reduction of the soluble TEAs occurs at the cytoplasmic membrane (CM), the location of the proton motive force-generating electron transport. However, in utilization of insoluble oxides, CM-localized electrons need to traverse the periplasm and the outer membrane (OM) to reach the extracellular matrix. Three mechanisms of transfer of OM-localized electrons to metal oxides have been hypothesized: (i) electron transfer through direct contact with the metal oxide, (ii) cyclic reduction/oxidation of electron shuttles, and (iii) solubilization of the metals with chelators, followed by diffusion to and across the OM to the CM. For a review of the proposed mechanisms, see reference 15.

While there are very few reports of bacteria producing chelators for DIR (51), there are more data to support the other two mechanisms. For example, using atomic force microscopy (AFM), Lower et al. (26) measured binding between both OM hemeproteins OmcA and MtrC and the iron oxide hematite and reported that OmcA shows a greater affinity toward hematite than does MtrC. These workers suggested that this tight binding is a prerequisite for direct electron transfer. Xiong et al. (55) also showed tight binding between OmcA and hematite by using dynamic light scattering and fluorescence correlation

* Corresponding author. Mailing address: 408 Althouse Laboratory, Department of Biochemistry and Molecular Biology, The Pennsylvania State University, University Park, PA 16802. Phone: (814) 863-1165. Fax: (814) 863-7024. E-mail: mxt3@psu.edu.

▽ Published ahead of print on 19 June 2009.

spectroscopy. Previous work in our laboratory (43, 44) demonstrating the rates of metal oxide reduction by membrane fractions from *Shewanella* also supported a direct-contact mechanism. Direct contact between cellular components and iron oxides is also consistent with the nanowire mechanism proposed by Gorby et al. (14).

In support of the electron shuttle hypothesis, two laboratories independently showed that *S. oneidensis* produces extracellular flavins, which may act as electron-shuttling agents (31, 52). The involvement of flavins as an electron shuttle would explain previous reports that *Shewanella* secretes a small, quinone-like compound involved in electron transfer (41) and can utilize sterically sequestered iron located in alginate beads (18).

While the previous studies described above provide compelling evidence for their respective mechanisms, none of the mechanisms have been subjected to detailed kinetic analysis. Kinetic studies, while not able to prove a mechanism, can be used to eliminate proposed mechanisms if rates of a reaction measured with purified enzymes, as determined in vitro, cannot account for the rates observed in whole cells. We previously described the importance of kinetic studies and how to apply these kinetic studies to DIR (6, 43, 44). Briefly, rate constants are determined by in vitro studies with purified enzymes. The kinetics of the enzyme of interest is then studied in the whole cell (or in subcellular fractions). The rate constants are then compared between these systems to determine whether the rate of the reactions catalyzed by the enzyme can account for the rates observed in the cell.

In our previous work, we performed kinetic studies on membrane fractions of *S. oneidensis* (43, 44). In the present study, this kinetic characterization is extended to purified enzymes and with whole cells for the purpose of determining kinetic competence. While our major focus is on the reduction of insoluble iron forms, for comparative purposes and as a control to validate our studies with the insoluble oxides, our study also includes a kinetic analysis of soluble chelated iron forms. We have focused our kinetic studies on two OM-localized hemeproteins, OmcA and MtrC. Previous genetic knockout studies show the importance of these enzymes in metal oxide reduction as potential terminal metal reductases (2, 35, 37). We describe both transient- and steady-state kinetic analyses. While both hemeproteins have been studied by stopped-flow analysis (48, 53) and by steady-state methods in whole cells (4), no study has yet attempted to infer mechanisms from scale-up kinetic studies (where kinetic constants from transient-state experiments are compared with those obtained from steady-state experiments). Our studies were thus performed at three different kinetic scales: (i) transient-state iron reduction using purified OmcA and MtrC, (ii) steady-state kinetics with purified total membrane (TM) fractions, and (iii) steady-state whole-cell kinetics.

MATERIALS AND METHODS

Materials. Xanthine oxidase from buttermilk, Triton X-100 SigmaUltra, ferric citrate, NTA [*N*,*N*-bis(carboxymethyl)glycine], and riboflavin were purchased from Sigma. 3-[(3-Cholamidopropyl)dimethylammonio]-1-propanesulfonate (CHAPS) was purchased from Soltec Ventures, Inc. EDTA was purchased from EMD Chemicals Inc.

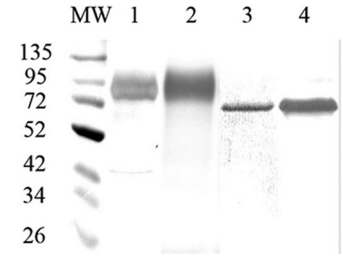

FIG. 1. SDS-PAGE of purified OmcA and MtrC. OmcA (lanes 1 and 2) and MtrC (lanes 3 and 4) were subjected to SDS-PAGE on 10% polyacrylamide and visualized by silver (lane 1), Coomassie blue (lane 3), or heme (lanes 2 and 4) staining. MW, molecular mass markers. Marker masses (in kilodaltons) are to the left of the gel.

Bacterial growth. *S. oneidensis* MR-1 (ATCC 700550) was maintained on Luria-Bertani (LB) agar. Single colonies were used to inoculate 5 ml of aerobic LB medium and then allowed to grow at 30°C to an optical density at 600 nm of 0.6. The culture was centrifuged at 10,000 × *g* for 15 min, and the pellet was washed with HEPES-buffered saline (0.7% NaCl in 10 mM HEPES, pH 7.4) and then resuspended in 1/10 of the volume of the same solution. This cell suspension (1 ml) was added to 4.5 liters of defined argon-purged M1 minimal medium as described by Myers and Nealson (36) and harvested when the ferrous ion concentration reached 35 mM (43).

TM isolation. The TM fraction was isolated according to Ruebush et al. (44) as modified from reference 34, by using lysozyme, EDTA, and 5% Brij.

OmcA and MtrC purification. TM (10 mg/ml) fractions were solubilized with 50 mM HEPES (pH 7.5)–5% Triton X-100 and subjected to anion-exchange chromatography (Q-Sepharose fast flow; Amersham) with a linear gradient of 0 to 100% buffer B at 1 ml/min over 160 min (buffer A = 50 mM HEPES [pH 7.5]–5% Triton X-100; buffer B = buffer A–0.5 M NaCl). The OmcA fraction, as determined by Western blot analysis, was isolated and subjected to MonoQ chromatography. OmcA was loaded onto a MonoQ column (Amersham) and eluted with a linear gradient of 0 to 100% buffer B at 1 ml/min over 160 min (buffer A = 50 mM HEPES [pH 7.5]–0.2% Triton X-100; buffer B = buffer A–0.5 M NaCl).

While the first heme peak (as detected by absorbance at 409 nm) contained OmcA, the second heme peak that eluted from the Q-Sepharose column contained the MtrC/A/B complex (42) as visualized by heme staining. To isolate MtrC from the purified complex, we first exchanged detergents by binding the complex to a Q-Sepharose column (Q-Sepharose fast flow; Amersham) and then washed with 3 column volumes of buffer A (50 mM HEPES [pH 7.5]–0.5% CHAPS). MtrC was eluted with a linear gradient of 0 to 100% buffer B at 1 ml/min over 160 min (buffer B = buffer A–0.5 M NaCl).

Extinction coefficients for OmcA and MtrC were determined with the pyridine hemochromogen assay (3). The extinction coefficient at 409 nm (ε_{409}) is 1,670,000 M^{-1} cm^{-1} for OmcA and 1,440,000 M^{-1} cm^{-1} for MtrC.

For standards in Western blot assays, recombinant MtrC was purified as inclusion bodies as previously described by Ross et al. (42). MtrC content in the purified inclusion bodies was determined by its UV absorbance associated with its aromatic amino acids. The ε_{276} (48,800 M^{-1} cm^{-1}) was determined as described by Edelhoch (10).

Transient-state kinetics. OmcA and MtrC were reduced enzymatically with xanthine oxidase (8). Stock solutions of xanthine oxidase (2 U/ml), xanthine (0.5 mM), and benzyl viologen (1 mM) were purged with oxygen-free argon and transferred to a Coy anaerobic chamber (3% hydrogen, N_2 atmosphere). Reaction mixtures contained purified OmcA (or MtrC) (0.5 μM), xanthine (0.15 mM), benzyl viologen (1.5 μM), and xanthine oxidase (0.01 U/ml).

Reduction was monitored by UV/Vis spectroscopy and was complete after approximately 2 h. Fully reduced protein was then loaded into an Applied Photosystems (Surrey, United Kingdom) SX.18MV stopped-flow apparatus. Heme oxidation was monitored with a diode array detector, and rates were obtained by monitoring the decrease in absorbance at 550 nm associated with ferroheme oxidation.

Western blot assay for quantification of MtrC and OmcA. Purified MtrC or OmcA was used as a protein standard for sodium dodecyl sulfate-polyacrylamide gel electrophoresis (SDS-PAGE)–Western blotting and ranged from 1.8×10^{-11} to 1.8×10^{-12} moles per lane. OmcA and MtrC were quantified in TM fractions (0.5 μg per lane) and whole cells (7.5 μl of cell suspension [2.25×10^7 total

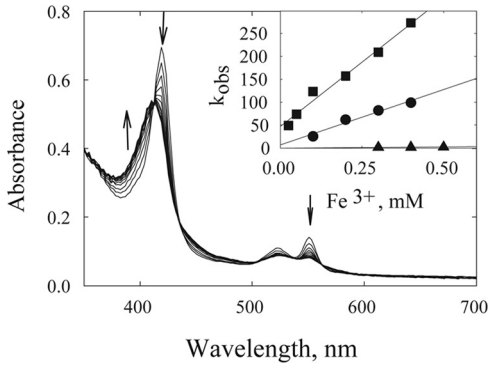

FIG. 2. Reaction of ferroOmcA with ferric iron chelates. The reaction of reduced OmcA (0.35 μM) with 0.1 mM NTA-Fe^{3+} was monitored by rapid scanning every 20 ms in a stopped-flow apparatus (total of 10 scans). Arrows indicate the direction of spectral change. (Inset) Plot of rate (k_{obs}) versus various concentrations of EDTA-Fe^{3+} (■), NTA-Fe^{3+} (●), and citrate-Fe^{3+} (▲).

cells]). After separation of the proteins by SDS-PAGE, the samples were transferred to a nitrocellulose membrane (Protran BA 83; Whatman) and protein bands were visualized with alkaline phosphatase-conjugated anti-rabbit immunoglobulin G and AP substrate (Immobilon Western; Millipore). Blots were then scanned and analyzed with ImageJ64 public software from NIH (http://rsbweb.nih.gov/ij/).

Iron reduction assays with whole cells and TM fractions. Reduction assays using TM fractions were performed as described previously (43, 44). Reaction mixtures contained 0.1 mg/ml TM protein, 10 mM formate, and Fe(III) forms as specified in the figure legends in 100 mM HEPES (pH 7.0). Reactions were initiated by addition of formate. At specified times, 100-μl aliquots were removed and quenched with 33 μl of 2 N HCl. Acidified samples (50 μl) were added to 950 μl of a ferrozine solution (1 g/liter ferrozine in 100 mM HEPES [pH 7]), and the ferrous ion concentration was determined spectrophotometrically at 562 nm by using an extinction coefficient of 27.9 mM^{-1} cm^{-1} (50).

Whole-cell experiments were identical to TM incubations, except that whole cells replaced the TM fraction. Isolation of whole cells was performed anaerobically at 4°C. The cells were centrifuged at 10,000 × *g* for 15 min. The cells were then washed with M1 minimal medium and suspended in 1/30 of the original volume of defined medium. From this stock, 100 μl (or 3×10^8 cells) was added to the iron reduction reaction mixtures.

In experiments in which spent medium was added (see below for spent medium preparation), either 450 or 900 μl was added to the reaction mixture.

Flavin quantification. TM fractions or whole cells were added to an equal volume of 5% (wt/vol) trichloracetic acid, mixed for 30 s, and placed on ice in the dark for 60 min. Samples were centrifuged at 10,000 × *g* for 12 min to pellet the precipitated protein, and the supernatant was analyzed by high-performance liquid chromatography (32). Samples were separated by reversed-phase liquid chromatography (HP 1090) with a Discovery C_{18} column (15 cm by 4.6 mm, 5 μm; Supelco) with a 2-cm guard column (Pelliguard LC-18; Supelco). Flavin content was determined by monitoring its associated fluorescence (HP 1046A programmable fluorescence detector) with an excitation wavelength of 440 nm and an emission wavelength of 525 nm (54). A gradient of methanol versus 20 mM ammonium acetate, pH 5.4, was used to determine the presence of flavin (52). The following gradient timetable was used to separate samples: 0 to 6 min (5% methanol), 6 to 28 min (increase from 5 to 37% methanol), 28 to 33 min (increase from 37 to 99% methanol), 33 to 35 min (hold at 99% methanol), and 35 to 36 min (rapid decrease from 99 to 5% methanol). Samples were analyzed for fluorescence at 440 nm with Chemstation (HP) and compared to a riboflavin standard (Sigma).

Spent medium preparation. After anaerobic cultures (described above) reached 35 mM Fe(II) and cells were removed, the spent ferric citrate medium was placed over a Chelex 100 resin column (100 to 200 mesh, sodium form; Bio-Rad) to remove any excess iron. The column was equilibrated with oxygen-free buffer (100 mM HEPES, pH 7.5) in the anaerobic chamber. Once the column was equilibrated, spent medium was added; collection started after 2 column volumes passed through the column.

Miscellaneous methods. Protein content was determined by the method of Lowry et al. (28) with bovine serum albumin as the standard. Goethite was synthesized by the method of Schwertmann and Cornell (46), and the Brunauer-Emmett-Teller surface area was estimated to be 33.9 m^2/g (7).

RESULTS

Purification of native OmcA and MtrC. For transient-state kinetic studies, OmcA and MtrC were purified from *S. oneidensis*. SDS-PAGE analysis showed that OmcA (Fig. 1A) was purified to greater than 95% homogeneity, as demonstrated by silver (Fig. 1A) or heme (Fig. 1B) staining. MtrC was equally pure (Coomassie blue, Fig. 1C; heme, Fig. 1D).

Transient-state kinetic studies of soluble iron forms with OmcA and MtrC. Kinetic constants between soluble iron and OmcA or MtrC were measured with a stopped-flow kinetic apparatus. Reaction rates were obtained by monitoring the change in absorbance at either 419 or 550 nm associated with the oxidation of ferroheme to ferriheme (Fig. 2). While both OmcA and MtrC contain 10 hemes/molecule, the data did not indicate significant differences in heme reactivity and thus the results were fitted with a single exponential. Rate constants were obtained from plots of observed rates versus Fe concentration: the slopes of linear fit lines are equal to forward rate constants (k_1), and the *y* intercepts are equal to the reverse rate constants (k_{-1}). The following reaction scheme depicts the interaction of reduced enzyme (ferroheme) with the oxidized iron chelate (encircled Fe^{3+}).

$$\text{Fe}^{3+} + \text{Ferroheme} \underset{k_{-1}}{\overset{k_1}{\rightleftharpoons}} \text{Fe}^{2+} \text{IIIIII Ferriheme}$$

Rate constants obtained for both OmcA and MtrC with the three ferric chelates citrate, NTA, and EDTA (Fig. 2) decreased in the order EDTA-Fe^{3+} > NTA-Fe^{3+} > citrate-Fe^{3+} (Tables 1 and 2).

Quantification of OmcA and MtrC. We previously performed steady-state kinetic analysis of iron reduction by membrane fraction and expressed rates as moles of Fe reduced per milligram of protein per minute (44). To obtain molecular rate constants from such studies (e.g., moles of Fe reduced per mol

TABLE 1. Kinetic constants for MtrC with soluble and insoluble iron forms[a]

Expt	Second-order rate constant (M^{-1} s^{-1}), mean ± SD			
	EDTA-Fe^{3+}	NTA-Fe^{3+}	Citrate-Fe^{3+}	Goethite
Purified enzyme	$9.2 \times 10^5 \pm 3.9 \times 10^4$	$2.4 \times 10^5 \pm 3.7 \times 10^4$	$3.9 \times 10^4 \pm 3.3 \times 10^3$	0.0099 ± 0.0007 (0.0033 ± 0.0003)[b]
TM	$1.9 \times 10^4 \pm 2.5 \times 10^3$	$1.3 \times 10^4 \pm 2.7 \times 10^3$	$1.2 \times 10^3 \pm 3.0 \times 10^2$	14.7 ± 2.7 (4.9 ± 0.9)
Whole cells	$9.0 \times 10^3 \pm 1.0 \times 10^3$	$1.1 \times 10^4 \pm 1.7 \times 10^3$	$6.7 \times 10^3 \pm 4.4 \times 10^2$	1.37 ± 0.17 (0.45 ± 0.05)

[a] See Materials and Methods for experimental details.
[b] The values in parentheses are in milliliters per square meter per second.

TABLE 2. Kinetic constants for OmcA with soluble and insoluble iron forms[a]

Expt	Second-order rate constant (M^{-1} s^{-1}), mean ± SD			
	EDTA-Fe^{3+}	NTA-Fe^{3+}	Citrate-Fe^{3+}	Goethite
Purified enzyme	$3.0 \times 10^5 \pm 7.4 \times 10^3$	$1.7 \times 10^5 \pm 2.9 \times 10^4$	$3.7 \times 10^4 \pm 3.2 \times 10^3$	0.019 ± 0.003 (0.0066 ± 0.001)[b]
TM	$1.5 \times 10^4 \pm 2.1 \times 10^3$	$1.4 \times 10^4 \pm 4.0 \times 10^3$	$1.2 \times 10^3 \pm 3.0 \times 10^2$	24.2 ± 5.5 (8.1 ± 1.8)
Whole cells	$9.2 \times 10^3 \pm 1.1 \times 10^3$	$1.1 \times 10^4 \pm 1.5 \times 10^3$	$7.0 \times 10^3 \pm 4.6 \times 10^2$	1.15 ± 0.2 (0.38 ± 0.07)

[a] See Materials and Methods for experimental details.
[b] The values in parentheses are in milliliters per square meter per second.

enzyme per min), the molar concentration of enzyme must be determined. Western blot assays with OmcA and MtrC standards were used to quantify the concentrations of these proteins in TM and whole-cell preparations. The specificity of these antibodies has been previously demonstrated (42). A sample Western blot of MtrC is shown in Fig. 3. Quantification by such methods yielded a concentration in TM preparations of $2.2 \times 10^{-10} \pm 2.5 \times 10^{-12}$ moles of OmcA and $1.9 \times 10^{-10} \pm 4.3 \times 10^{-12}$ moles of MtrC per mg of TM protein. For whole cells, our Western blot assays yielded $7.9 \times 10^{-20} \pm 9.5 \times 10^{-21}$ moles of OmcA and $1.2 \times 10^{-19} \pm 4.5 \times 10^{-20}$ moles of MtrC per cell, which is similar to what was determined by Borloo et al. (4) (4×10^{-21} moles of OmcA per cell) based on the heme content of OmcA and MtrC mutants.

Kinetic analysis of iron reduction. Iron reduction kinetic studies were performed with both soluble and insoluble forms of iron. The electron donor for in vitro TM incubations was formate. For in vivo whole-cell incubations, the electron donor was the same as the carbon source used for growth, lactate. The reaction kinetics were fitted to the Michaelis-Menten equation to determine K_m, k_{cat}, and k_{cat}/K_m for EDTA-Fe^{3+}, NTA-Fe^{3+}, and citrate-Fe^{3+} and either TM (Fig. 4A) or whole cells (Fig. 4B). K_m is the half-saturation constant, k_{cat} is the maximal velocity (V_{max}) expressed as turnover number, and k_{cat}/K_m is the apparent second-order rate constant or catalytic efficiency of the enzyme, which can be experimentally determined by the slope at low substrate concentrations for a plot of rate versus substrate concentration. By quantifying the amounts of OmcA and MtrC in these preparations, the velocities could be expressed as a turnover number: moles of Fe^{2+} produced per second per mole of either MtrC or OmcA (thus simplifying to units of s^{-1}). Figure 4 shows data only for OmcA (the MtrC-normalized velocity plots are similar and therefore not shown). The second-order rate constants (k_{cat}/K_m) are listed in Table 2. For the TM fraction, k_{cat}/K_m values obtained with the soluble iron form followed the same trend as that observed from stopped-flow experiments: EDTA-Fe^{3+} > NTA-Fe^{3+} > citrate-Fe^{3+}. For whole cells, EDTA-Fe^{3+} and NTA-Fe^{3+} exhibited similar k_{cat}/K_m values, which were greater than those of citrate-Fe^{3+}.

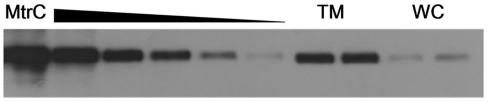

FIG. 3. Western blot analysis of MtrC standard, TM, and whole cells (WC). MtrC content was visualized by using affinity-purified polyclonal antibodies to MtrC. MtrC protein standard amounts ranged from 1.8×10^{-11} to 1.8×10^{-12} moles and were subjected to 10% SDS-PAGE along with TM fractions (0.5 μg per lane) and whole-cell samples (7.5 μl of cell suspension [2.25×10^7 total cells]).

Steady-state kinetic experiments were also performed with goethite and either TM fractions or whole cells (Fig. 5). Quantification of OmcA and MtrC by Western blot analysis allowed calculation of k_{cat}/K_m expressed as per mole or per unit of surface area of goethite. The k_{cat}/K_m values, expressed per mole of goethite (formula, FeOOH), are much lower than the values calculated per mole of Fe for the soluble-Fe experiments (Tables 1 and 2).

Single-turnover experiments were also performed with goethite. Again, OmcA and MtrC were reduced with xanthine oxidase and the reactions with goethite were monitored by heme oxidation at 550 nm. These reactions are much slower than the reaction with the soluble iron forms, yielding much slower second-order rate constants. Furthermore, of significance, the rate constants (k_{cat}/K_m) are up to 3 orders of magnitude lower than the rate constants obtained from steady-state experiments with TM or whole cells (Tables 1 and 2).

Flavin content of ferric-citrate-grown cultures. Because flavins (flavin adenine dinucleotide, flavin mononucleotide, and riboflavin) have been proposed to act as the shuttling agent for iron oxide reduction (52), we investigated whether flavins were produced in ferric citrate-grown cultures. Total flavin content was measured by high-performance liquid chromatography separation and its associated fluorescence. The flavin concentrations of whole cells, TM preparation, and spent culture medium, respectively, were 0.38 ± 0.058, 0.12 ± 0.018, and 5.8 ± 0.70 μmol of flavin/g of protein. The flavin concentration of the extracellular medium (spent culture supernatant with cells removed) was measured to be 0.30 ± 0.02 μM. When calculated per gram of whole-cell protein, our value of 0.38 μmol of flavin/g of protein is within the error range of the value of 0.4 μmol/g of protein measured by von Canstein et al. (52) for fumarate-grown cultures of *Shewanella*. Because the flavin in the extracellular medium has been hypothesized to act as an electron shuttle, we also analyzed whether our TM fraction contained flavin: 0.12 μmol of flavin per g of protein was measured in the TM fractions. This is perhaps not surprising due to the hydrophobic nature of flavins and the likelihood of membrane association. It follows that flavin was found in washed whole cells as well. The percentage that was extracellular could not be determined.

Flavin-dependent stimulation of goethite reduction. To assess whether the flavin-containing medium could stimulate iron reduction, we examined the effect of adding spent medium containing the low-molecular-weight redox-active fraction to our iron-reducing reaction mixtures. The spent medium was first passed through a Chelex column to remove all of the

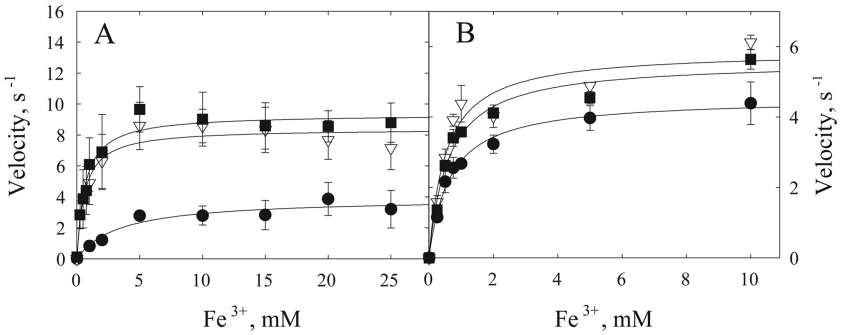

FIG. 4. Steady-state kinetic analysis of soluble iron reduction. Rates of TM-mediated (A) and whole-cell-mediated (B) iron reduction are expressed as moles of iron reduced per mole of OmcA per second (simplifying to s^{-1}). TM fractions (0.1 mg/ml) or whole-cell suspensions (see Materials and Methods) were added to 1-ml reaction mixtures containing buffer or defined medium and the specified concentrations of chelated iron species. The reaction was initiated upon the addition of 100 μl of 100 mM formate or 100 μl of the cell suspension. At 0, 15, and 30 min, 100-μl aliquots were removed and analyzed for ferrous iron (nanomoles of Fe^{2+} formed per minute per milligram of TM). Panel A shows results from TM incubations, and panel B shows results from whole-cell incubations with EDTA-Fe^{3+} (■), NTA-Fe^{3+} (▽), or citrate-Fe^{3+} (●). Note the difference in scale between panels A and B.

soluble iron and added back to whole-cell incubations. Addition of Chelex-treated spent culture medium caused a 10-fold increase in the rate of goethite reduction. The iron reduction rates of whole cells resuspended in defined medium (defined M1 mineral medium), both defined and spent media, and spent medium alone were 0.033 ± 0.007, 0.18 ± 0.016, and 0.32 ± 0.058 mmol of Fe^{2+}/min/g of protein, respectively. Similar stimulation was observed with the TM fraction (data not shown).

Reaction of riboflavin with OmcA and MtrC. The reaction of OmcA or MtrC with riboflavin was studied by stopped-flow analysis. Similar to studies using soluble iron, the rate of decrease in absorbance at 550 nm was used to monitor the oxidation of ferroheme to ferriheme. The second-order rate constants for OmcA and MtrC measured in the presence of riboflavin were 5.9×10^5 and 1.2×10^5 M^{-1} s^{-1}, respectively.

We then determined the reactivity of flavins with goethite. Riboflavin was reduced by the xanthine oxidase system, and its reaction with goethite was monitored by the increase in absorbance at 450 nm associated with oxidized flavin. These single-turnover experiments performed at different goethite concentrations yielded a second-order rate constant of 0.22 M^{-1} s^{-1}.

Simulation of transient- and steady-state rates with calculated rate constants. Our results suggest that the sluggish reactivity between OmcA and MtrC with goethite can be compensated for by the introduction of flavin into the mechanism. To further assess the role of flavins in whole-cell-catalyzed DIR, we performed some additional experiments with flavin for the purpose of kinetic simulations. As described above, we monitored the oxidation of OmcA by goethite, except that this time we added flavin at a physiologically relevant concentration (Fig. 6). The added flavin increased the rate of OmcA oxidation. The data were then simulated by using Kinsim and our experimentally determined rate constants (Fig. 6). The simulation showed that our rate constants are able to fit the data at three different concentrations of goethite with satisfactory accuracy.

We then simulated steady-state results from whole-cell ex-

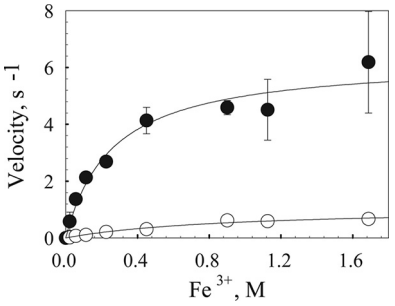

FIG. 5. Steady-state kinetic analysis of iron oxide reduction. TM (●)- and whole-cell (○)-mediated goethite reduction rates are expressed as moles of Fe^{2+} per mole of OmcA per second. TM fractions (0.1 mg/ml) or whole-cell suspensions (100 μl) were added to 1-ml reaction samples containing buffer or defined medium and various concentrations of goethite. The reaction was initiated upon the addition of 100 μl of 100 mM formate or 100 μl of the cell suspension, and 100-μl aliquots were taken at 0, 15, and 30 min for Fe^{2+} quantification.

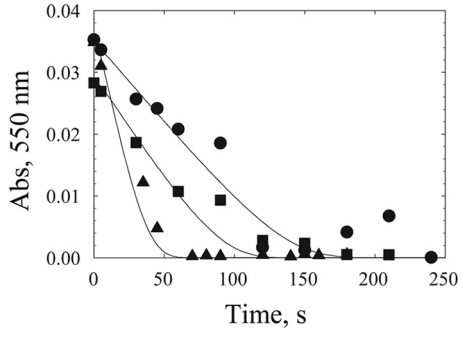

FIG. 6. Kinetic simulation of OmcA-mediated reduction of goethite in the presence of riboflavin. The reaction was monitored by measuring the oxidation of ferroOmcA as absorbance (Abs) at 550 nm. Data points are from experiments with 0.47 μM ferroOmcA, 1 μM flavin, and various concentrations of goethite, i.e., 21 (●), 34 (■), and 113 (▲) mM. Lines represent simulated data for the reaction mechanism shown in Fig. 8A with rate constants of 5.9×10^5 M^{-1} s^{-1} for OmcA and flavin and 0.22 M^{-1} s^{-1} for flavin and goethite, reactant concentrations of 0.476 μM OmcA and 1 μM riboflavin, and the three goethite amounts indicated above.

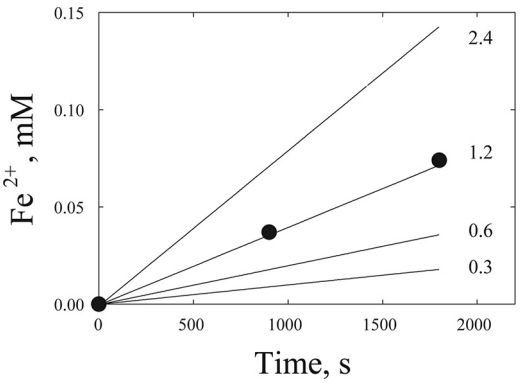

FIG. 7. Simulation of steady-state whole-cell-mediated goethite reduction by using experimentally determined rate constants for OmcA and riboflavin (5.9×10^5 M^{-1} s^{-1}) and for riboflavin and goethite (0.22 M^{-1} s^{-1}). Points (●) are experimental data from experiments measuring Fe^{2+} formation in whole-cell incubations with goethite (10 mg/ml). Reaction conditions were as described in Materials and Methods. Lines represent simulated rates of Fe^{2+} formation at various flavin concentrations (micromolar). The concentration of OmcA used in the simulation is the same as the concentration in the actual experiment (8.6×10^{-8} M). See Fig. 8B for the mechanism used in the simulation.

periments by using a flavin-dependent mechanism. The simulation was performed by using a range of flavin concentrations slightly higher than our measured value of 0.30 μM for bulk phase. We reasoned that the effective concentration of flavin in proximity to the cell would be higher than that measured in the bulk phase. As shown in Fig. 7, by using our experimentally determined rate constants for individual steps of electron transfer between OmcA and flavin and between flavin and goethite, a concentration of 1.35 μM flavin perfectly simulated the time course of iron reduction by whole cells.

DISCUSSION

Of the three proposed mechanisms for DIR of metal oxides, (i) direct contact, (ii) redox shuttles, and (iii) metal chelators, the first two have received the most attention. Experimental evidence for direct contact as the route of electron transfer first came from AFM studies by Lower et al. (27). These workers were able to show preferential binding of goethite to whole *Shewanella* cells that were anaerobically—as opposed to aerobically—grown. The AFM force curves suggested the involvement of a 150-kDa protein which they referred to as the "putative reductase" critical for such binding. More recently, Lower et al. (26) again used AFM to study the interaction of OmcA and MtrC with hematite. They showed that the OmcA-hematite interaction is twice the strength of the MtrC-hematite interaction and proposed that such strong binding interactions allowed for direct electron transfer to the iron oxide TEA. The direct-contact mechanism was also supported by a study by Xiong et al. (55) using dynamic light scattering and fluorescence correlation spectroscopy to measure the binding affinity between OmcA and hematite. Also, using NADH as the electron donor, they measured a maximal activity of 60 nmol of Fe^{2+} mg of $OmcA^{-1}$ min^{-1} for the reduction of hematite by OmcA. Recent work in our laboratory using an in vitro model system of purified TM fractions (44) is also consistent with the direct-contact mechanism. We proposed that the most likely mechanism for insoluble iron reduction would be direct contact since we assumed that small molecules would be removed from the TM sample after centrifugation and dialysis. Another study in support of a direct-contact mechanism for *Shewanella* involves nanowires (14). While the identity of the terminal reductase in the nanowires has yet to be identified, implicit in the arguments for this mechanism is direct contact between the nanowire and the metal oxide.

The possible involvement of secreted electron shuttles in the reduction of poorly soluble minerals was first proposed by Newman and Kolter (41). Experimental evidence, although indirect, for the participation of electron shuttles in DIR by dissimilatory Fe(III)-reducing microorganisms was further examined by the work of Nevin and Lovley (40). They were able to show reduction of iron oxide trapped in porous alginate beads. In a similar experiment, Lies et al. (18) demonstrated reduction of iron (hydr)oxides precipitated in nanoporous glass beads by *S. oneidensis* MR-1. These studies demonstrated the phenomenology of electron transfer without direct contact, but more substantive evidence was not provided until very recently. Two groups independently provided chemical evidence for the production of extracellular flavins as redox mediators by *S. oneidensis* (31, 52). They showed that addition of flavin increased the rate of goethite reduction but had no effect on soluble iron reduction. One concern over the use of electron shuttles is energetic efficiency: unless used for many cycles of electron transfer, the energy expended to synthesize a flavin molecule may be greater than that returned. Marsili et al. (31) argued that accumulation of flavins in *Shewanella* biofilms increased the transfer of electrons to an electrode by 370%, while the energy required to produce the observed levels of flavins was <0.1% of the total cellular ATP produced at that oxidation current. In order to produce 250 nM flavin over 72 h, it would potentially cost the cell 6.7×10^{-3} μmol of ATP/mg of protein/h (31).

Lacking in all of the above studies are supportive kinetic analyses. In expounding the virtue of kinetic analysis, Cleland (9) stated that kinetics should be the final arbiter of mechanistic studies. The scale-up kinetic studies described here were performed to identify the physiologically relevant mechanisms by using the criteria of kinetic competence. Such scale-up studies, while difficult, can also identify relevant factors that contribute to catalysis at the different scales (pure enzymes, cell fractions, whole cells) and should lead toward a better understanding of how to make predictions for natural systems. The limitations of such studies (6) are briefly described below.

To scale from steady-state kinetics, one must use the Michaelis-Menten equation

$$v = \frac{V_{\max}[S]}{K_m + [S]}$$

while for whole cells, data are generally fitted to the Monod equation

$$\frac{d[S]}{dt} = \frac{-(\mu_{\max}/Y)X[S]}{K + [S]}$$

Here, [*S*] is the concentration of the rate-limiting substrate, $\mu_{\max}$ is the maximum specific growth rate, *Y* is the growth yield

coefficient, X is the biomass concentration, and K is the half-saturation constant for growth. Scaling up from purified enzymes to membrane fractions to whole cells requires comparison of these two equations, both of which are only valid under selected conditions. For example, cell viability is important in whole-cell studies because substrate toxicity, cell growth, and cell death will impact the Monod fits. If the kinetic analsysis can be performed in a short time span, under nongrowth conditions (where no cell growth occurs and Xa is constant), the Monod equation has the same form as the Michaelis-Menten equation. In that case, V_{max} is equal to $(\mu max/Y)Xa$ and V_{max}/K_m is equal to the slope of the Monod plot (nongrowth conditions with whole cells). At low substrate concentrations, the slope of both curves is an indicator of the kinetic response of the system to the substrate concentration. Also, such a response is only valid in whole cells when the substrate of interest can be manipulated. Such is the case with extracellular enzymes OmcA and MtrC described in this study. To determine rate constants, the concentration of the enzyme must be known (yielding k_{cat} and the second-order rate constant). Hence, our determination of OmcA and MtrC concentrations by Western blot assays.

If involved in physiologically relevant catalysis, kinetic constants obtained from transient-state studies should be as fast as or faster than the overall steady-state rates of membrane fractions and these rates, in turn, must be as fast as or faster than the overall whole-culture rates (9, 21). When rates cannot be scaled up to account for catalysis in membrane fractions or whole cells (i.e., the transient-state rates with purified enzymes are too slow to account for rates at steady state), either the enzyme of interest is not involved in catalysis or its involvement is not in accordance with the proposed mechanism (6).

Reduction of soluble ferric species. While our present study was designed mainly to address the mechanism of electron transfer to insoluble metal oxides, we also studied the soluble iron chelates as a control for comparison and to validate our studies with the metal oxides. Past research in our laboratory and others has shown that soluble TEAs can be reduced in the periplasm at the CM (44). Nevertheless, OM hemeproteins are capable of efficiently reducing chelated ferric species (53). The rate constants obtained here with OmcA and MtrC and EDTA-Fe^{3+}, NTA-Fe^{3+}, and citrate-Fe^{3+} are comparable to values obtained by Wang et al. (53) with reactivities in the order EDTA-Fe^{3+} > NTA-Fe^{3+} > citrate-Fe^{3+}. The rate constants obtained from the stopped-flow experiments are faster than those obtained from the TM or whole cells. Furthermore, the rate constant with each ferric chelate is within 1 order of magnitude for each scale, an acceptable error given the reproducibility of our experiments.

It is noteworthy that our studies with whole cells and the transient-state analysis of NTA-Fe^{3+} yielded rate constants lower by 2 to 3 orders of magnitude than those calculated by Borloo et al. (4). In their study, they quantified OmcA and MtrC by SDS-PAGE and heme staining of the gels. This difference may be due to differences in incubation and assay conditions. Borloo et al. (4) used fumarate as the TEA, while we used ferric citrate. We have shown that ferric citrate-grown cells produce up to 19 times more heme than do fumarate-grown cells. Also, in contrast to our study, Borloo and coworkers included ferrozine in the reaction mixture while we added ferrozine after the reaction had been quenched with acid. This may impact the rate of iron reduction. While it may be difficult to compare our whole-cell kinetic constants with those of Borloo et al. (4), our rate constants obtained from stopped-flow analysis are very similar to those determined by Wang et al. (53). Both results are consistent with OmcA and MtrC being kinetically competent to catalyze soluble iron reduction by direct contact.

The ability to extrapolate steady-state rates from transient-state rate constants is difficult even with purified enzymes (11). Extrapolation from pure enzymes to whole cells is even more problematic. However, as described below, such an exercise, in which data are simulated with a mechanism and measured rate constants, can be valuable in eliminating proposed mechanisms.

Reduction of insoluble iron oxide. Scale-up kinetics of soluble iron yielded rate constants within approximately 1 order of magnitude from purified enzymes to TM and whole cells. As discussed above, the rate constants obtained at all three scales for the soluble electron acceptors are therefore consistent with the conclusion that OmcA and MtrC are kinetically competent. In contrast, scale-up studies with goethite clearly show that OmcA and MtrC cannot participate in iron oxide reduction through direct contact alone: the rate constants for OmcA and MtrC with goethite are 2 to 3 orders of magnitude lower than the rates obtained with whole cells or TM fractions. The inability to simulate or account for steady-state results unequivocally eliminates the mechanism related to direct contact between the hemeproteins and the iron oxide for this organism. This result reaffirms what biochemists have long known: formal binding of a substrate (formation of a ternary complex) is not a prerequisite for catalysis (e.g., ribulose 1,5-diphosphate carboxylase has no formal binding site for CO_2 or O_2 [5, 16]; also, the Theorell-Chance mechanism [13] should be considered). In other words, while OmcA or MtrC may bind tightly to the iron oxide substrate (26, 55), this does not necessarily imply anything about the kinetics of particulate iron oxide reduction.

The other hypothesized mechanism invoking direct contact is electron transfer through putative nanowires (14). Our results do not allow us to comment on the involvement of nanowires. Nanowires have been reported to be produced by *Shewanella* under microanaerobic conditions (14). The present study was not performed under such conditions and in fact was performed under electron acceptor-rich conditions. Therefore, nanowires are not involved in the experimental results discussed here.

Reduction of flavins. The inability to kinetically account for goethite reduction by OmcA or MtrC could be resolved by inclusion of flavin in the reaction mechanism. Consistent with previously published results (52), we were able to stimulate goethite reduction with flavins. Addition of Chelex-treated spent culture medium stimulated goethite reduction by whole cells. If, indeed, electron transfer by direct contact is too slow to account for catalysis, it would follow that the TM fraction and whole cells (which had been centrifuged and washed) should not have yielded rate constants faster than those obtained with purified OmcA and MtrC. However, we found that despite multiple centrifugation steps, the TM still contained flavins. This residual flavin can then participate in electron transfer and account for the higher rate constants obtained

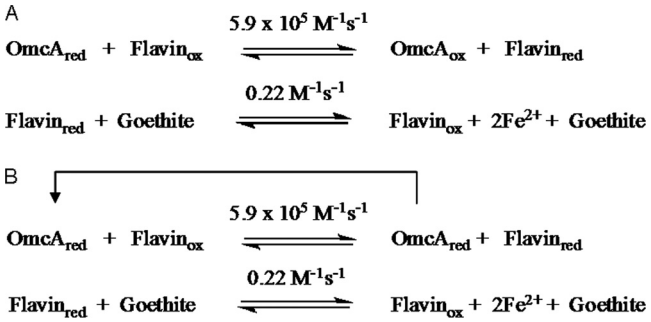

FIG. 8. (A) Mechanism used for simulation of single-turnover experiments for OmcA/flavin goethite reduction shown in Fig. 6. The rate constants were experimentally determined. Flavin reduction by OmcA occurs very fast, followed by a slower reduction of goethite by flavin. (B) Mechanism used for simulation of whole-cell-mediated goethite reduction shown in Fig. 7. To simulate multiple-turnover (steady-state) data in the linear part of the Michaelis-Menten curve (where iron is limiting and not saturating), OmcA was kept reduced, thereby ensuring that the rate of OmcA reduction was not rate limiting.

with the TM. While we also found flavins in washed whole cells, our data do not allow us to distinguish between extracellular and intracellular flavins. The whole cells, resuspended in fresh growth medium, would presumably be actively synthesizing and secreting flavins, which would stimulate iron oxide reduction. There remains the possibility that flavins are found in the extracellular medium not due to active secretion but by inadvertent loss from a flavoprotein. While this possibility cannot be eliminated by the results of our study, we argue that this is unlikely simply due to the high concentration of flavin found in the extracellular medium. Extracellular flavin mononucleotide and riboflavin concentrations were found to be 30 times higher than intracellular concentrations (52). It is difficult to envision *Shewanella* being so energetically inefficient through the loss of essential prosthetic groups.

If flavins are part of the kinetic mechanism, then the k_{cat}/K_m values determined from our steady-state experiments with TM fractions and whole cells are not true second-order rate constants between goethite and OmcA or MtrC. They are apparent rate constants obtained with flavin acting as a shuttle. This is substantiated by our kinetic simulations of steady-state data from whole cells. Using a mechanism involving flavin mediation, the experimentally determined rate constants and the experimentally determined concentrations of OmcA and flavin, we were able to simulate the steady-state data. Our proposed mechanism for OmcA and MtrC reduction of goethite is shown in Fig. 8. The validity of the mechanism shown along with the concentration of hemeprotein and flavin and with the rate constants is supported by the kinetic simulation shown in Fig. 6 and 7.

Conclusions. Using the concept of kinetic competence and scale-up kinetic analysis, we have attempted to determine the mechanism of OM electron transfer for *Shewanella*. Scale-up kinetics dictates that the rates of individual steps in a mechanism must be just as fast as or faster than the overall steps in a pathway. Accurate scale-up is difficult; the number of variables contributing to rates of a reaction increases significantly as one goes up in scale on the kinetic ladder. Our scale-up kinetic studies showed, for the first time, the following. (i) Within experimental error, reduction of soluble iron forms can be scaled up from isolated-enzyme to whole-cell experiments by using the concentration of enzyme in each experiment; this implies that OmcA and MtrC can account for the catalysis of soluble iron in whole cells (i.e., kinetic competence has been demonstrated). (ii) OmcA and MtrC are not kinetically competent to account for physiological goethite reduction via direct contact because the relevant rate constants are 3 orders of magnitude too slow. (iii) When flavins are added into the kinetic mechanism, the reaction rates are greatly increased and can therefore account for the reduction of insoluble iron oxides in vivo.

Thus, of the three possible mechanisms used by *Shewanella* to transfer electrons to insoluble Fe oxides—direct contact (26, 55), electron shuttle (31, 52), and chelation (51)—our data have eliminated direct contact as a plausible mechanism of electron transfer from OmcA or MtrC to iron oxides and are consistent with the involvement of electron shuttles in DIR. Flavins are particularly implicated.

ACKNOWLEDGMENTS

This research was supported by the NSF Environmental Molecular Sciences Institute program (CHE-0431328) through the Penn State Center for Environmental Kinetics Analysis and by DOE grant ER64399 0013153. Funding for D. Ross derived partially from the Penn State Biogeochemical Research Initiative for Education (BRIE) sponsored by NSF (IGERT) (NSF DGE-9972759). We acknowledge conversations with J. Zachara and E. Roden as facilitated by funding from DOE OBER as part of the Center for Environmental Kinetics Analysis.

We thank Laura Liermann and Aaron Regberg for help in the synthesis of goethite. Some of the stopped-flow experiments were performed in the laboratory of Marty Bollinger (Penn State University). We thank one of the reviewers for the suggestions that flavins are lost from a critical OM flavoprotein and that stimulation occurs from conversion of the apoprotein to the holoprotein.

REFERENCES

1. **Anderson, R. T., H. A. Vrionis, I. Ortiz-Bernad, C. T. Resch, P. E. Long, R. Dayvault, K. Karp, S. Marutzky, D. R. Metzler, A. Peacock, D. C. White, M. Lowe, and D. R. Lovley.** 2003. Stimulating the in situ activity of *Geobacter* species to remove uranium from the groundwater of a uranium-contaminated aquifer. Appl. Environ. Microbiol. **69:**5884–5891.
2. **Beliaev, A. S., D. A. Saffarini, J. L. McLaughlin, and D. Hunnicutt.** 2001. MtrC, an outer membrane decahaem *c* cytochrome required for metal reduction in *Shewanella putrefaciens* MR-1. Mol. Microbiol. **39:**722–730.
3. **Berry, E. A., and B. L. Trumpower.** 1987. Simultaneous determination of hemes a, b, and c from pyridine hemochrome spectra. Anal. Biochem. **161:** 1–15.
4. **Borloo, J., B. Vergauwen, L. De Smet, A. Brige, B. Motte, B. Devreese, and J. Van Beeumen.** 2007. A kinetic approach to the dependence of dissimilatory metal reduction by *Shewanella oneidensis* MR-1 on the outer membrane cytochromes *c* OmcA and OmcB. FEBS J. **274:**3728–3738.
5. **Bowes, G., and W. L. Ogren.** 1972. Oxygen inhibition and other properties of soybean ribulose 1,5-diphosphate carboxylase. J. Biol. Chem. **247:**2171–2176.
6. **Brantley, S. L., S. Ruebush, J.-H. Jang, and M. Tien.** 2006. Analysis of (bio)geochemical kinetics of Fe III oxides, p. 79–116. *In* P. A. Maurice and L. A. Warren (ed.), Methods for study of microbe mineral interactions. Clay Minerals Society workshop lectures series, vol. 14. The Clay Minerals Society, Chantilly, VA.
7. **Brunauer, S.** 1987. About some critics of the bet theory. Langmuir **3:**3–4.
8. **Cheng, Z., L. D. Arscott, D. P. Ballou, and C. H. Williams, Jr.** 2007. The relationship of the redox potentials of thioredoxin and thioredoxin reductase from Drosophila melanogaster to the enzymatic mechanism: reduced thioredoxin is the reductant of glutathione in Drosophila. Biochemistry **46:**7875–7885.
9. **Cleland, W. W.** 1975. Partition analysis and concept of net rate constants as tools in enzyme kinetics. Biochemistry **14:**3220–3224.
10. **Edelhoch, H.** 1967. Spectroscopic determination of tryptophan and tyrosine in proteins. Biochemistry **6:**1948–1954.

11. **Fierke, C. A., K. A. Johnson, and S. J. Benkovic.** 1987. Construction and evaluation of the kinetic scheme associated with dihydrofolate reductase from *Escherichia coli*. Biochemistry **26:**4085–4092.
12. **Fredrickson, J. K., H. M. Kostandarithes, S. W. Li, A. E. Plymale, and M. J. Daly.** 2000. Reduction of Fe(III), Cr(VI), U(VI), and Tc(VII) by *Deinococcus radiodurans* R1. Appl. Environ. Microbiol. **66:**2006–2011.
13. **Gates, C. A., and D. B. Northrop.** 1988. Alternative substrate and inhibition kinetics of aminoglycoside nucleotidyltransferase 2″-I in support of a Theorell-Chance kinetic mechanism. Biochemistry **27:**3826–3833.
14. **Gorby, Y. A., S. Yanina, J. S. McLean, K. M. Rosso, D. Moyles, A. Dohnalkova, T. J. Beveridge, I. S. Chang, B. H. Kim, K. S. Kim, D. E. Culley, S. B. Reed, M. F. Romine, D. A. Saffarini, E. A. Hill, L. Shi, D. A. Elias, D. W. Kennedy, G. Pinchuk, K. Watanabe, S. Ishii, B. Logan, K. H. Nealson, and J. K. Fredrickson.** 2006. Electrically conductive bacterial nanowires produced by *Shewanella oneidensis* strain MR-1 and other microorganisms. Proc. Natl. Acad. Sci. USA **103:**11358–11363.
15. **Gralnick, J. A., and D. K. Newman.** 2007. Extracellular respiration. Mol. Microbiol. **65:**1–11.
16. **Gutteridge, S., M. A. J. Parry, C. N. G. Schmidt, and J. Feeney.** 1984. An investigation of ribulosebisphosphate carboxylase activity by high-resolution H-1-NMR. FEBS Lett. **170:**355–359.
17. **Klonowska, A., T. Heulin, and A. Vermeglio.** 2005. Selenite and tellurite reduction by *Shewanella oneidensis*. Appl. Environ. Microbiol. **71:**5607–5609.
18. **Lies, D. P., M. E. Hernandez, A. Kappler, R. E. Mielke, J. A. Gralnick, and D. K. Newman.** 2005. *Shewanella oneidensis* MR-1 uses overlapping pathways for iron reduction at a distance and by direct contact under conditions relevant for biofilms. Appl. Environ. Microbiol. **71:**4414–4426.
19. **Liu, C. X., Y. A. Gorby, J. M. Zachara, J. K. Fredrickson, and C. F. Brown.** 2002. Reduction kinetics of Fe(III), Co(III), U(VI) Cr(VI) and Tc(VII) in cultures of dissimilatory metal-reducing bacteria. Biotechnol. Bioeng. **80:** 637–649.
20. **Liu, C. X., B. H. Jeon, J. M. Zachara, Z. M. Wang, A. Dohnalkova, and J. K. Fredrickson.** 2006. Kinetics of microbial reduction of solid phase U(VI). Environ. Sci. Technol. **40:**6290–6296.
21. **Lorimer, G. H., M. R. Badger, and T. J. Andrews.** 1976. The activation of ribulose-1,5-bisphosphate carboxylase by carbon dioxide and magnesium ions. Equilibria, kinetics, a suggested mechanism, and physiological implications. Biochemistry **15:**529–535.
22. **Lovley, D. R.** 1993. Dissimilatory metal reduction. Annu. Rev. Microbiol. **47:**263–290.
23. **Lovley, D. R., D. E. Holmes, and K. P. Nevin.** 2004. Dissimilatory Fe(III) and Mn(IV) reduction. Adv. Microb. Physiol. **49:**219–286.
24. **Lovley, D. R., and E. J. Phillips.** 1992. Reduction of uranium by *Desulfovibrio desulfuricans*. Appl. Environ. Microbiol. **58:**850–856.
25. **Lovley, D. R., and E. J. P. Phillips.** 1988. Novel mode of microbial energy metabolism organic carbon oxidation coupled to dissimilatory reduction of iron or manganese. Appl. Environ. Microbiol. **54:**1472–1480.
26. **Lower, B. H., L. Shi, R. Yongsunthon, T. C. Droubay, D. E. McCready, and S. K. Lower.** 2007. Specific bonds between an iron oxide surface and outer membrane cytochromes MtrC and OmcA from *Shewanella oneidensis* MR-1. J. Bacteriol. **189:**4944–4952.
27. **Lower, S. K., M. F. Hochella, and T. J. Beveridge.** 2001. Bacterial recognition of mineral surfaces: nanoscale interactions between *Shewanella* and α-FeOOH. Science **292:**1360–1363.
28. **Lowry, O. H., N. J. Rosebrough, A. L. Farr, and R. J. Randall.** 1951. Protein measurement with the Folin phenol reagent. J. Biol. Chem. **193:**265–275.
29. **Madigan, M. T., J. M. Martinko, and J. Parker.** 2000. Brock biology of microorganisms. Prentice Hall, Englewood Cliffs, NJ.
30. **Marshall, M. J., A. S. Beliaev, A. C. Dohnalkova, D. W. Kennedy, L. Shi, Z. Wang, M. I. Boyanov, B. Lai, K. M. Kemner, J. S. McLean, S. B. Reed, D. E. Culley, V. L. Bailey, C. J. Simonson, D. A. Saffarini, M. F. Romine, J. M. Zachara, and J. K. Fredrickson.** 2006. *c*-type cytochrome-dependent formation of U(IV) nanoparticles by *Shewanella oneidensis*. PLoS Biol. **4:**e268.
31. **Marsili, E., D. B. Baron, I. D. Shikhare, D. Coursolle, J. A. Gralnick, and D. R. Bond.** 2008. *Shewanella* secretes flavins that mediate extracellular electron transfer. Proc. Natl. Acad. Sci. USA **105:**3968–3973.
32. **Midttun, Ø., S. Hustad, E. Solheim, J. Schneede, and P. M. Ueland.** 2005. Multianalyte quantification of vitamin B_6 and B_2 species in the nanomolar range in human plasma by liquid chromatography-tandem mass spectrometry. Clin. Chem. **51:**1206–1216.
33. **Moser, D. P., and K. H. Nealson.** 1996. Growth of the facultative anaerobe *Shewanella putrefaciens* by elemental sulfur reduction. Appl. Environ. Microbiol. **62:**2100–2105.
34. **Myers, C. R., and J. M. Myers.** 1992. Localization of cytochromes to the outer membrane of anaerobically grown *Shewanella putrefaciens* MR-1. J. Bacteriol. **174:**3429–3438.
35. **Myers, C. R., and J. M. Myers.** 2004. The outer membrane cytochromes of *Shewanella oneidensis* MR-1 are lipoproteins. Lett. Appl. Microbiol. **39:**466–470.
36. **Myers, C. R., and K. H. Nealson.** 1988. Microbial reduction of manganese oxides interactions with iron and sulfur. Geochim. Cosmochim. Acta **52:** 2727–2732.
37. **Myers, J. M., and C. R. Myers.** 2003. Overlapping role of the outer membrane cytochromes of *Shewanella oneidensis* MR-1 in the reduction of manganese(IV) oxide. Lett. Appl. Microbiol. **37:**21–25.
38. **Nealson, K. H., and J. F. Banfield (ed.).** 1997. Geomicrobiology: interactions between microbes and minerals. Mineralogical Society of America, Washington, DC.
39. **Nealson, K. H., A. Belz, and B. McKee.** 2002. Breathing metals as a way of life: geobiology in action. Antonie van Leeuwenhoek **81:**215–222.
40. **Nevin, K. P., and D. R. Lovley.** 2002. Mechanisms for Fe(III) oxide reduction in sedimentary environments. Geomicrobiol. J. **19:**141–159.
41. **Newman, D. K., and R. Kolter.** 2000. A role for excreted quinones in extracellular electron transfer. Nature **405:**94–97.
42. **Ross, D. E., S. S. Ruebush, S. L. Brantley, R. S. Hartshorne, T. A. Clarke, D. J. Richardson, and M. Tien.** 2007. Characterization of protein-protein interactions involved in iron reduction by *Shewanella oneidensis* MR-1. Appl. Environ. Microbiol. **73:**5797–5808.
43. **Ruebush, S. S., S. L. Brantley, and M. Tien.** 2006. Reduction of soluble and insoluble iron forms by membrane fractions of *Shewanella oneidensis* grown under aerobic and anaerobic conditions. Appl. Environ. Microbiol. **72:**2925–2935.
44. **Ruebush, S. S., G. A. Icopini, S. L. Brantley, and M. Tien.** 2006. In vitro enzymatic reduction kinetics of mineral oxides by membrane fractions from *Shewanella oneidensis* MR-1. Geochim. Cosmochim. Acta **70:**56–70.
45. **Sani, R. K., B. M. Peyton, J. E. Amonette, and G. G. Geesey.** 2004. Reduction of uranium(VI) under sulfate-reducing conditions in the presence of Fe(III)-(hydr)oxides. Geochim. Cosmochim. Acta **68:**2639–2648.
46. **Schwertmann, U., and R. M. Cornell.** 1991. Iron oxides in the laboratory: preparation and characterization, p. 137. *In* R. M. Cornell and U. Schwertmann (ed.), The iron oxides: structure, properties, reactions, occurrences and uses. John Wiley, John & Sons, Inc., New York, NY.
47. **Shelobolina, E. S., M. V. Coppi, A. A. Korenevsky, L. N. DiDonato, S. A. Sullivan, H. Konishi, H. F. Xu, C. Leang, J. E. Butler, B. C. Kim, and D. R. Lovley.** 2007. Importance of *c*-type cytochromes for U(VI) reduction by *Geobacter sulfurreducens*. BMC Microbiol. **7:**16.
48. **Shi, L., B. Chen, Z. Wang, D. A. Elias, M. U. Mayer, Y. A. Gorby, S. Ni, B. H. Lower, D. W. Kennedy, D. S. Wunschel, H. M. Mottaz, M. J. Marshall, E. A. Hill, A. S. Beliaev, J. M. Zachara, J. K. Fredrickson, and T. C. Squier.** 2006. Isolation of a high-affinity functional protein complex between OmcA and MtrC: two outer membrane decaheme *c*-type cytochromes of *Shewanella oneidensis* MR-1. J. Bacteriol. **188:**4705–4714.
49. **Shi, L., T. C. Squier, J. M. Zachara, and J. K. Fredrickson.** 2007. Respiration of metal (hydr)oxides by Shewanella and Geobacter: a key role for multihaem *c*-type cytochromes. Mol. Microbiol. **65:**12–20.
50. **Stookey, L. L.** 1970. Ferrozine: a new spectrophotometric reagent for iron. Anal. Chem. **42:**779–781.
51. **Taillefert, M., J. S. Beckler, E. Carey, J. L. Burns, C. M. Fennessey, and T. J. DiChristina.** 2007. *Shewanella putrefaciens* produces an Fe(III)-solubilizing organic ligand during anaerobic respiration on insoluble Fe(III) oxides. J. Inorg. Biochem. **101:**1760–1767.
52. **von Canstein, H., J. Ogawa, S. Shimizu, and J. R. Lloyd.** 2008. Secretion of flavins by *Shewanella* species and their role in extracellular electron transfer. Appl. Environ. Microbiol. **74:**615–623.
53. **Wang, Z., C. Liu, X. Wang, M. J. Marshall, J. M. Zachara, K. M. Rosso, M. Dupuis, J. K. Fredrickson, S. Heald, and L. Shi.** 2008. Kinetics of reduction of Fe(III) complexes by outer membrane cytochromes MtrC and OmcA of *Shewanella oneidensis* MR-1. Appl. Environ. Microbiol. **74:**6746–6755.
54. **Woodcock, E. A., J. J. Warthesen, and T. P. Labuza.** 1982. Riboflavin photochemical degradation in pasta measured by high performance liquid chromatography. J. Food Sci. **47:**545–555.
55. **Xiong, Y., L. Shi, B. Chen, M. U. Mayer, B. H. Lower, Y. Londer, S. Bose, M. F. Hochella, J. K. Fredrickson, and T. C. Squier.** 2006. High-affinity binding and direct electron transfer to solid metals by the *Shewanella oneidensis* MR-1 outer membrane *c*-type cytochrome OmcA. J. Am. Chem. Soc. **128:**13978–13979.